NASA-CR-193726

IN-32-CR

180 871

p. 20

Recursive Time-Varying Filter Banks for Subband Image Coding[1]

Mark J. T. Smith and Wilson C. Chung

Georgia Institute of Technology

School of Electrical Engineering

Atlanta, Georgia 30332

Abstract

Filter banks and wavelet decompositions that employ recursive filters have been considered previously and are recognized for their efficiency in partitioning the frequency spectrum. This paper presents an analysis of a new infinite impulse response (IIR) filter bank in which these computationally efficient filters may be changed adaptively in response to the input. The filter bank is presented and discussed in the context of finite-support signals with the intended application in subband image coding.

In the absence of quantization errors, exact reconstruction can be achieved and by the proper choice of an adaptation scheme, it is shown that IIR time-varying filter banks can yield improvement over conventional ones.

1   Introduction

Subband image coding is a well-known technique in which an input is split into a small number of subband images, each of which is associated with a different region in the spatial frequency plane. The subband images are decimated to their Nyquist rates prior to being quantized and coded. In reconstruction the images are decoded, upsampled, and then merged together. The process in which the input is split and merged is called analysis/synthesis. There are many performance and systems related design issues associated with analysis/synthesis as discussed in [2], [4], [7] and elsewhere. Recursive analysis and synthesis filter banks have been shown to be particularly attractive because they can be designed to reconstruct the input exactly in the absence of coding and can achieve tremendous computational efficiency relative to comparable FIR systems [4], [5]. These filter banks are typically two-band systems that serve as building blocks for uniform and non-uniform band tree structured systems. However, parallel form recursive filter banks have also been shown to work well [11]. In such a case, the subband images are complex valued.

Thus to avoid increasing the data rate, Hermitian symmetry is exploited to counter the sample increase due to the presence of complex numbers in the subband images.

When subbands are quantized, distortion results and the degree of the distortion is inversely proportional to the bit rate. The quantization noise generates three types of interrelated distortions:

1. *Aliasing.* This is due to the partial loss of aliasing cancellation in the synthesis section that arises from quantization. It appears subjectively as blurring in the reconstructed images.

2. *Ringing distortion.* This appears as amplitude oscillations (or ringing) in the vicinity of edges in the image. As discussed in [4], its cause may be directly related to the ripples in the step response characteristics of the analysis/synthesis filters.

3. *In-band spectral distortion.* This distortion is attributed to the deviation in the spectral magnitude and phase of subband images excluding the inter-band effects of aliasing and ringing. In essence, this form of distortion accounts for all remaining deviations when aliasing and ringing effects are removed.

Much attention has been given to minimizing the perceptually important coding distortions in image coding systems. For low bit rate subband image coding systems, aliasing and ringing distortions are often cited as being objectionable. Efforts to reduce these effects have been considered previously but with limited success [4], [5], [12]. The difficulty is that the ripples of the step response of the filters, which are the source of the ringing distortion, are needed to achieve good filter magnitude response characteristics. Good spectral magnitude characteristics are important for reducing the effects of aliasing in the presence of coding. Aliasing distortion appears as blurring in the image and is subjectively noticeable. If filters with good magnitude characteristics are used to reduce the aliasing, then ringing distortion results that is noticeable and objectionable. As to which is worse is a matter of opinion. It is clear, however, that the elimination or reduction of both is desirable. This dilemma is a consequence of the Gibbs Phenomenon which implies that is it impossible to have filter banks with good (i.e. monotonic) step response characteristics and good magnitude response characteristics within the conventional paradigm. However, it is possible to overcome this seemingly fundamental difficulty by using time varying filter banks as we shall see. The first introduction of the concept of time-varying filter banks appears in [3] and is based on the time domain theory and design methodology presented in [15], [14], and [13]. The approach taken in [3] has some attractive features: time-varying capability is conceptually simple in this framework and system delay can be controlled very easily. On the other side of the coin, the approach is inherently limited to FIR systems and the system design task can be difficult for practical filters.

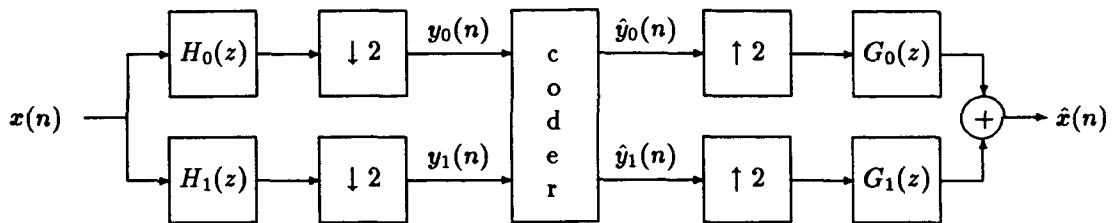In this paper, we introduce the concept of time-varying *recursive* filter banks and demonstrate

Figure 1: Two-Band Analysis/Synthesis System

that they provide the additional degree of freedom that allows them to overcome the step-response-magnitude-response constraint associated with the Gibbs Phenomenon. We derive the conditions under which we can switch between filters of desirable properties. Furthermore, this new time-varying recursive filter preserves the exact reconstruction property and maintains very high computational efficiency. We presented this idea at the 1992 DSP Workshop [16] and discussed some of the analysis issues at the 1992 Asilomar Conference [17]; both [16] and [17] are rather limited due to page length constraints.[2]

This paper begins with a discussion of the exact reconstruction IIR filter bank after which the time-varying conditions are derived. The equations for time-varying analysis/synthesis are derived and a design strategy is developed that allows for much improved performance over conventional filter banks.

2 Exact Reconstruction IIR Filter Banks

The starting point for this work is the two-band analysis/synthesis system shown in Figure 1 where $\{H_0(z), H_1(z)\}$ and $\{G_0(z), G_1(z)\}$ are the pairs of lowpass/highpass analysis/synthesis filters. The analysis filters have the form:

$$H_0(z) = P_0(z^2) + z^{-1}P_1(z^2) \tag{1}$$

$$H_1(z) = P_0(z^2) - z^{-1}P_1(z^2) \tag{2}$$

and may be implemented using the well-known polyphase structure shown in Figure 2 where $P_0(z)$ and $P_1(z)$ are the analysis polyphase filters and $Q_0(z)$ and $Q_1(z)$ are the synthesis polyphase filters.

The exact reconstruction property of this recursive filter bank is evident from an examination of the polyphase structure. Observe that the criss-cross networks in the analysis and synthesis sections of Figure 2 are simply two-point DFT butterflies and that the cascade of the two

---

[2]The authors recently became aware of similar work developed independently in Norway by Husoy and Aase [18].
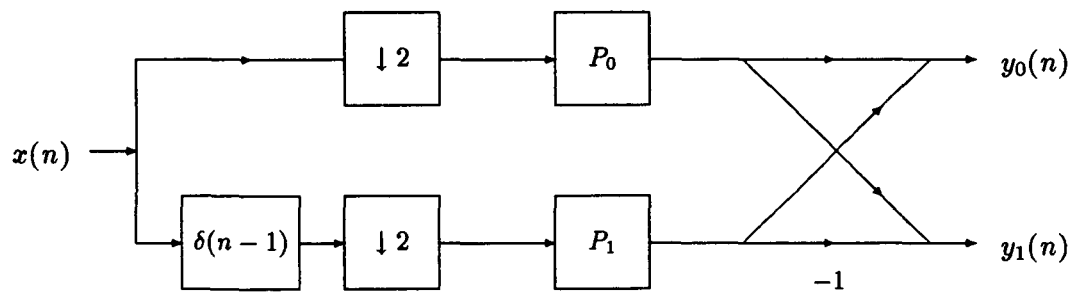
(a) Analysis
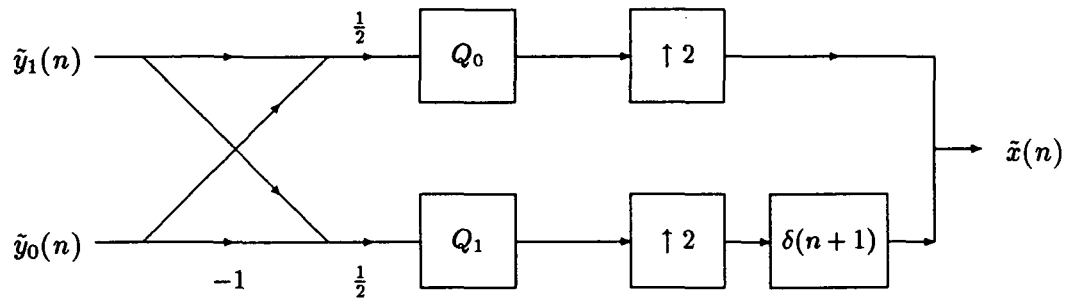
(b) Synthesis

Figure 2: Two-Band Polyphase Implementation of the Analysis/Synthesis System
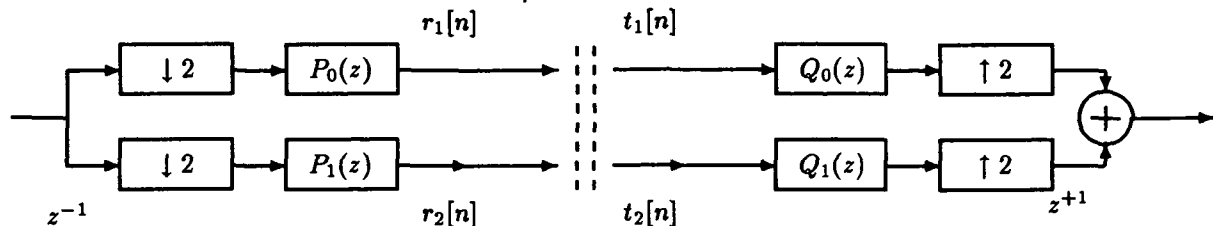
Figure 3: Two-Band Polyphase Implementation with DFT Butterflies Omitted

results in an identity system. Therefore the combined analysis/synthesis polyphase system can be simplified as shown in Figure 3. By inspecting Figure 3, it is clear that if

$$Q_0(z) = \frac{1}{P_0(z)} \quad \text{and} \quad Q_1(z) = \frac{1}{P_1(z)},$$

then the overall system reduces to an identity system and hence the reconstruction is exact. A few points are noteworthy in this regard. First, $P_0(z)$ and $P_1(z)$ are assumed to be causal stable recursive filters with zeros strictly outside the unit circle and have allpass or near allpass characteristics. Second, by definition, the synthesis polyphase filters $Q_0(z)$ and $Q_1(z)$ will have their poles outside the unit circle and their zeros inside the circle. Consequently, they are anti-causal and stable. Third, because the image boundaries are finite in length, the circular convolution method discussed in [4] is used to handle the analysis and reconstruction at the image boundaries in order to avoid an increase in the subband data. It should be noted that the recursive polyphase filters are well-behaved and do not attempt to invert stopbands or magnify selected regions of the spectrum that might lead to adverse emphasis of coding noise [4]. Comparisons were given to systems based on linear-phase FIR filters and to those based on linear-phase and non-linear-phase IIR filters. The interested reader is directed to this reference [4] for further details.

3 The New Time-Varying IIR Filter Banks

In this section, we derive a new variant of the IIR filter bank in which the coefficients of the constituent filters are allowed to vary with time. The coefficients of the polyphase filters $P_0(z)$ and $P_1(z)$ are selectively changed at some point in the filtering process to another set of polyphase filters. This process of changing the filters allows us to improve the coding performance. The problem we address in this section is how to reconstruct without distortion once we have switched the filter coefficients. By examining the simplified polyphase structure in Figure 3, it is apparent that it is sufficient to determine the conditions under which $r_i[n] = t_i[n]$ for $i = 1, 2$. Clearly if we can guarantee that $r_i[n] = t_i[n]$ at all times before, during, and after switching the coefficients, then exact reconstruction is also guaranteed.

To illustrate the analysis and reconstruction problem, consider the graphical illustration shown in Figure 4. Assume that the impulse response $p_L[n]$ shown in the figure corresponds to

that of a causal, stable analysis polyphase filter

$$P_L(z) = \frac{\alpha_0^L + \alpha_1^L z^{-1} + \cdots + \alpha_{M_0}^L z^{-M_0}}{1 + \beta_1^L z^{-1} + \beta_2^L z^{-2} + \cdots + \beta_{N_0}^L z^{-N_0}}.$$

At time $n = 0$, the filter is changed to $p_R[n]$ corresponding to a new polyphase filter

$$P_R(z) = \frac{\alpha_0^R + \alpha_1^R z^{-1} + \cdots + \alpha_{M_1}^R z^{-M_1}}{1 + \beta_1^R z^{-1} + \beta_2^R z^{-2} + \cdots + \beta_{N_1}^R z^{-N_1}}.$$

The labels L and R signify that the signal or filter coefficient is associated with the left and right halves of the time index, respectively.

3.1   Time Domain Analysis

The direct form difference equations that implement the polyphase filters are:

$$v_L[n] = \sum_{m=0}^{M_0} \alpha_m^L x[n-m] - \sum_{\ell=1}^{N_0} \beta_\ell^L v_L[n-\ell] \qquad -\infty < n \le -1 \tag{3}$$

and

$$v_R[n] = \sum_{m=0}^{M_1} \alpha_m^R x[n-m] - \sum_{\ell=1}^{N_1} \beta_\ell^R v_R[n-\ell] \qquad 0 \le n < \infty \tag{4}$$

Here, $v_L[n]$ and $v_R[n]$ are the left-sided and right-sided components of the output $v[n]$, i.e. $v[n] = v_L[n] + v_R[n]$. In addition, equation (4) requires the initial conditions $v_R[-N_1]$, $v_R[-N_1 - 1]$, ..., $v_R[-1]$ in order to evaluate $v_R[0]$ since

$$v_R[0] = \sum_{m=0}^{M_1} \alpha_m^R x[-m] - \sum_{\ell=1}^{N_1} \beta_\ell^R v_R[-\ell] \tag{5}$$

Rather than making these initial conditions zero, which effectively discards the recent history of the input, we assume the more desirable initial conditions

$$v_R[n] = v_L[n] \quad \text{in the range} \quad -N_1 \le n \le -1.$$

Generalizing the reconstruction procedure discussed in [4] for conventional recursive filter banks, we obtain the reconstruction shown in Figure 5 which is based on anti-causal filtering. Here $q_R[n]$ and $q_L[n]$ are impulse responses corresponding to the stable, anti-causal polyphase synthesis filters. The corresponding difference equations are

$$x_R[n-A] = \frac{1}{-\alpha_{M_1}^R} \sum_{\ell=1}^{M_1} \alpha_{M_1-\ell}^R x_R[n+\ell-A] + \frac{1}{\alpha_{M_1}^R} \sum_{m=0}^{N_1} \beta_{N_1-m}^R v_R[n+m-B] \tag{6}$$

for $0 \le n < \infty$ and

$$x_L[n-C] = \frac{1}{-\alpha_{M_0}^L} \sum_{\ell=1}^{M_0} \alpha_{M_0-\ell}^L x_L[n+\ell-C] + \frac{1}{\alpha_{M_0}^L} \sum_{m=0}^{N_0} \beta_{N_0-m}^L v_L[n+m-D] \tag{7}$$
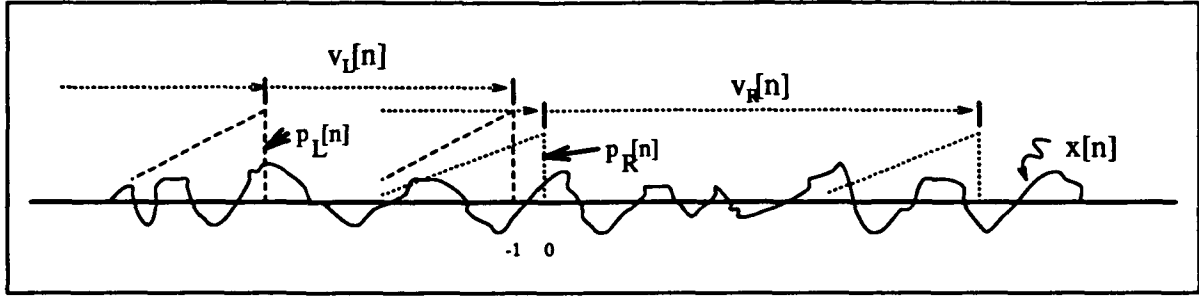
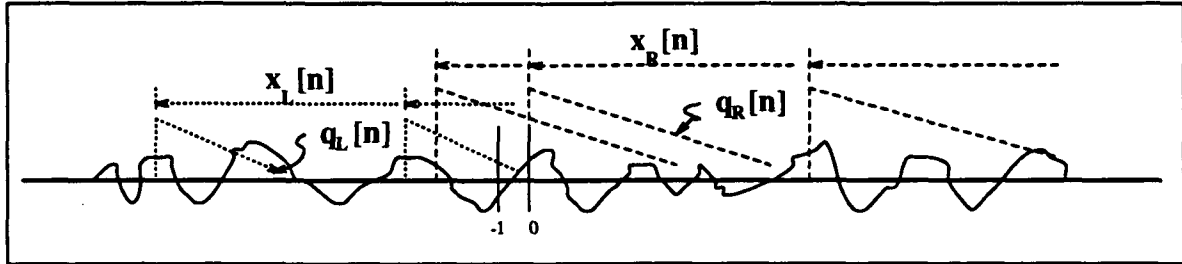Figure 4: Graphical Illustration of Time-Varying IIR Analysis Polyphase Filtering

Figure 5: Graphical Illustration of Time-Varying IIR Synthesis Polyphase Filtering

for $-\infty < n \le -1$, where A, B, C, and D are arbitrary integer shift constants. The reconstruction sections, $x_R[n]$ and $x_L[n]$ are right-sided and left-sided components of the reconstructed signal $x[n]$, as shown in Figure 5 and have the property that

$$x[n] = x_R[n] + x_L[n]. \tag{8}$$

Although the form of the reconstruction is given by equations (3- 7), the unknown parameters A, B, C, and D must be determined.

3.2   z-Transform Domain Analysis

In this section, we determine the exact reconstruction conditions under this new time-varying filter bank paradigm (i.e. find A, B, C, and D) and show explicitly that reconstruction is exact. The time-varying filter bank problem can be analyzed in the z-transform domain in terms of a causal and anti-causal unilateral z-transform. We define the causal unilateral z-transform as

$$X_R(z) = \sum_{n=0}^{\infty} x[n]z^{-n} \tag{9}$$

and the anti-causal unilateral z-transform as

$$X_L(z) = \sum_{n=-\infty}^{-1} x[n]z^{-n}. \tag{10}$$

The sum of $X_R(z)$ and $X_L(z)$ is identical to the bilateral z-transform of $x[n]$. These causal and anti-causal transforms have shift properties associated with them that may be described in the following way. Suppose that n_0 is an integer and $u[n]$ is the unit step function. Then, for a time

shift of n_0 in $x[n]$

$$w[n] = x[n - n_0]$$

the causal unilateral z-transform $W_R(z)$ is

$$W_R(z) = z^{-n_0}X_R(z) + \sum_{\ell=0}^{n_0-1} x[\ell - n_0]z^{-\ell}u[n_0 - 1] - z^{-n_0}\sum_{\ell=0}^{-n_0-1} x[\ell]z^{-\ell}u[-n_0 - 1]. \qquad (11)$$

Similarly, for the anti-causal z-transform, the same time shift

$$w[n] = x[n - n_0]$$

results in the anti-causal transform

$$W_L(z) = z^{-n_0}X_L(z) - z^{-n_0}\sum_{\ell=1}^{n_0} x[-\ell]z^{\ell}u[n_0 - 1] + z^{-n_0}\sum_{\ell=0}^{-n_0-1} x[\ell]z^{-\ell}u[-n_0 - 1]. \qquad (12)$$

This shift property will be used to take the transforms of the analysis equations (3) and (4) and the synthesis equations (6) and (7). A derivation of this shift property is given in appendix A.

Using the causal and anti-causal z-transforms and their corresponding shift properties, we can take the z-transforms of the analysis and synthesis equations. The transform properties allow us to model the initial conditions explicitly for the point at which we switch the filter coefficients. In this analysis, we assume that we switch the filter coefficients at $n = 0$.

For convenience in taking the transform, we express equation (4) as

$$\sum_{\ell=0}^{N_1}\beta_\ell^R v_R[n - \ell] = \sum_{m=0}^{M_1}\alpha_m^R x[n - m] \qquad 0 \le n < \infty \qquad (13)$$

(where $\beta_0^R = 1$) and compute its z-transform using the definition (9) and shift property (11). We obtain

$$\sum_{\ell=0}^{N_1}\beta_\ell^R z^{-\ell}V_R(z) + \sum_{\ell=1}^{N_1}\beta_\ell^R\sum_{k=0}^{\ell-1} v_R[k - \ell]z^{-k} = \sum_{m=0}^{M_1}\alpha_m^R X_R(z)z^{-m} + \sum_{m=1}^{M_1}\alpha_m^R\sum_{\ell=0}^{m-1} x_R[\ell - m]z^{-\ell}. \qquad (14)$$

Next we can write the right-sided synthesis equation (equation (6)) as

$$\sum_{\ell=0}^{M_1} x_R[n + \ell - A]\alpha_{M_1-\ell}^R = \sum_{m=0}^{N_1}\beta_{N_1-m}^R v_R[n + m - B] \qquad (15)$$

and take its z-transform to obtain

$$\sum_{\ell=0}^{M_1}\alpha_{M_1-\ell}^R X_R(z)z^{\ell-A} + \sum_{\ell=0}^{M_1}\alpha_{M_1-\ell}^R\left(\sum_{m=0}^{A-\ell-1} x_R[m - A + \ell]z^{-m}u[A - \ell - 1]\right.$$

$$\left. - z^{-A+\ell}\sum_{m=0}^{-A+\ell-1} x_R[m]u[-A + \ell - 1]\right)$$

$$= \sum_{m=0}^{N_1}\beta_{N_1-m}^R V_R(z)z^{m-B} + \sum_{m=0}^{N_1}\beta_{N_1-m}^R\left(\sum_{\ell=0}^{B-m-1} v_R[\ell - B + m]z^{-\ell}u[B - m - 1]\right.$$

$$- z^{B-m} \sum_{\ell=0}^{-B+m-1} v_R[\ell]u[-B+m-1]). \tag{16}$$

This is the z-transform of the synthesis equation for the right-sided sequence $x_R[n]$. If the right and left sides of this equation can be shown to be identical, then we have shown exact reconstruction for $x_R[n]$. To explicitly show that the equality holds, we must express $V_R(z)$ in terms of $X_R(z)$, the initial conditions, and the filter coefficients. Using equation (14), we can remove the $V_R(z)$ term by substituting

$$z^{N_1-B}\left(\sum_{m=0}^{M_1}\alpha_m^R X_R(z)z^{-m} + \sum_{m=1}^{M_1}\alpha_m^R\sum_{\ell=0}^{m-1} x_R[\ell-m]z^{-\ell} - \sum_{\ell=1}^{N_1}\beta_\ell^R\sum_{k=0}^{\ell-1}v_R[k-\ell]z^{-k}\right) \tag{17}$$

for

$$\sum_{m=0}^{N_1}\beta_{N_1-m}^R V_R(z)z^{m-B}$$

in equation (16). After the substitution, equation (16) becomes

$$\underbrace{\sum_{\ell=0}^{M_1}\alpha_{M_1-\ell}^R X_R(z)z^{\ell-A}}_{(1)} + \underbrace{\sum_{\ell=0}^{M_1}\alpha_{M_1-\ell}^R\sum_{m=0}^{A-\ell-1} x_R[m-A+\ell]z^{-m}u[A-\ell-1]}_{(2)}$$

$$\underbrace{-\sum_{\ell=0}^{M_1}\alpha_{M_1-\ell}^R z^{-A+\ell}\sum_{m=0}^{-A+\ell-1} x_R[m]u[-A+\ell-1]}_{(3)}$$

$$= \underbrace{z^{N_1-B}\sum_{m=0}^{M_1}\alpha_m^R X_R(z)z^{-m}}_{(4)} + \underbrace{z^{N_1-B}\sum_{m=1}^{M_1}\alpha_m^R\sum_{\ell=0}^{m-1} x_R[\ell-m]z^{-\ell}}_{(5)} - \underbrace{z^{N_1-B}\sum_{\ell=1}^{N_1}\beta_\ell^R\sum_{k=0}^{\ell-1}v_R[k-\ell]z^{-k}}_{(6)}$$

$$+ \underbrace{\sum_{m=0}^{N_1}\beta_{N_1-m}^R\sum_{\ell=0}^{B-m-1} v_R[\ell-B+m]z^{-\ell}u[B-m-1]}_{(7)} - \underbrace{\sum_{m=0}^{N_1}\beta_{N_1-m}^R z^{B-m}\sum_{\ell=0}^{-B+m-1} v_R[\ell]u[-B+m-1]}_{(8)}$$

$$\tag{18}$$

By examining this equation, it becomes apparent that we can group like terms and that there must be equivalence within these groups in order for the equality to hold. Consider, first, terms 6, 7, and 8, which are the only terms containing $v_R[n]$ components. The sum of these terms must be zero, i.e.

$$\underbrace{-z^{N_1-B}\sum_{\ell=1}^{N_1}\beta_\ell^R\sum_{k=0}^{\ell-1}v_R[k-\ell]z^{-k}}_{(6)} + \underbrace{\sum_{m=0}^{N_1}\beta_{N_1-m}^R\sum_{\ell=0}^{B-m-1} v_R[\ell-B+m]z^{-\ell}u[B-m-1]}_{(7)}$$

$$\underbrace{-\sum_{m=0}^{N_1}\beta_{N_1-m}^R z^{B-m}\sum_{\ell=0}^{-B+m-1} v_R[\ell]u[-B+m-1]}_{(8)} = 0 \tag{19}$$

At initial glance, it is apparent that cancellation can only occur between either terms 6 and 7 or 7 and 8 because these are the only combinations in which the signs are opposite. A closer examination shows that terms 7 and 8 are disjoint in the variable m due to the $u[B - m - 1]$ and $u[-B + m - 1]$ terms. Thus, it is sufficient to focus on terms 6 and 7. In term 6, if we let $\ell = N_1 - m$ we obtain

$$-z^{N_1-B}\sum_{m=0}^{N_1-1}\beta_{N_1-m}^R \sum_{k=0}^{N_1-m-1} v_R[k - N_1 + m]z^{-k}$$

which cancels with term 7 when $B = N_1$. Moreover, when $B = N_1$, term 8 disappears because $u[-B + m - 1]$ goes to zero.

We can now group terms 1 and 4 together in equation (18) because only they contain the $X_R(z)$ components. Letting $\ell = M_1 - m$ in term 1, we obtain

$$\sum_{m=0}^{M_1}\alpha_m^R X_R(z)z^{M_1-m-A}.$$

This becomes identical to term 4 when $A = M_1$, resulting in cancellation.

The only remaining terms are 2, 3, and 5. Immediately we observe that term 3 is zero. Note that because $A = M_1$, the $u[-A + \ell - 1]$ forces term 3 to be zero. Thus all that is left is to show that terms 2 and 5 cancel. Letting $\ell = M_1 - n$ in term 2, we obtain

$$\sum_{n=0}^{M_1}\alpha_n^R \sum_{m=0}^{n-1} x_R[m - n]z^{-m}u[n - 1] = \sum_{n=1}^{M_1}\alpha_n^R \sum_{m=0}^{n-1} x_R[m - n]z^{-m}$$

which is equivalent to term 5. Thus we see that when $A = -M_1$ and $B = -N_1$, we can exactly reconstruct $x_R[n]$.

What remains is to prove that we can reconstruct $x_L[n]$. The same procedure can be applied to the left-sided equations. In particular, the analysis equation (3) can be written as

$$\sum_{\ell=0}^{N_0}\beta_\ell^L v_L[n - \ell] = \sum_{m=0}^{M_0}\alpha_m^L x[n - m] \tag{20}$$

where $\beta_0^L = 1$. Its corresponding z-transform is

$$\sum_{\ell=0}^{N_0}\beta_\ell^L z^{-\ell}V_L(z) - \sum_{\ell=0}^{N_0}\beta_\ell^L z^{-\ell}\sum_{k=1}^{\ell} v_L[-k]z^k u[\ell - 1] = \sum_{m=0}^{M_0}\alpha_m^L z^{-m}X_L(z) - \sum_{m=0}^{M_0}\alpha_m^L z^{-m}\sum_{\ell=1}^{m} x_L[-\ell]z^\ell u[m - 1] \tag{21}$$

The z-transform for the left-sided synthesis equation (7) is

$$\sum_{\ell=0}^{M_0}\alpha_{M_0-\ell}^L X_L(z)z^{\ell-C} - \sum_{\ell=0}^{M_0}\alpha_{M_0-\ell}^L z^{\ell-C}\left(\sum_{k=1}^{C-\ell} x_L[-k]z^k u[C - \ell - 1] + \sum_{k=0}^{\ell-C-1} x_L[k]z^{-k}u[\ell - C - 1]\right) =$$
$$\sum_{m=0}^{N_0}\beta_{N_0-m}^L z^{m-D}V_L(z) - \sum_{m=0}^{N_0}\beta_{N_0-m}^L z^{m-D}\left(\sum_{\ell=1}^{D-m} v_L[-\ell]z^\ell u[D - m - 1] + \sum_{\ell=0}^{-D+m-1} v_L[\ell]z^{-\ell}u[m - D - 1]\right) \tag{22}$$

Applying equation (21) to equation (22), we can remove the $V_L(z)$ components and we obtain

$$\sum_{\ell=0}^{M_0} \alpha_{M_0-\ell}^L X_L(z) z^{\ell-C} - \sum_{\ell=0}^{M_0} \alpha_{M_0-\ell}^L z^{\ell-C} \left(\sum_{k=1}^{C-\ell} x_L[-k] z^k u[C-\ell-1] \right.$$

$$\left. + \sum_{k=0}^{\ell-C-1} x_L[k] z^{-k} u[\ell-C-1] \right) =$$

$$z^{N_0-D} \left(\sum_{\ell=0}^{N_0} \beta_\ell^L z^{-\ell} \sum_{k=1}^{\ell} v_L[-k] z^k u[\ell-1] + \sum_{m=0}^{M_0} \alpha_m^L z^{-m} X_L(z) \right.$$

$$- \sum_{m=0}^{M_0} \alpha_m^L z^{-m} \sum_{\ell=1}^{m} x_L[-\ell] z^\ell u[m-1] \right) - \sum_{m=0}^{N_0} \beta_{N_0-m}^L z^{m-D}$$

$$\left(\sum_{\ell=1}^{D-m} v_L[-\ell] z^\ell u[D-m-1] + \sum_{\ell=0}^{-D+\ell-1} v_L[\ell] z^{-\ell} u[m-D-1] \right) \tag{23}$$

Again we can equate like terms and solve for the unknowns. Doing so, we find $C = M_0$ and $D = N_0$, and consequently prove that $x_L[n]$ may be exactly reconstructed.

4 Results

The time-varying filter bank reconstruction problem shares similarities with conventional inverse polyphase reconstruction. However, the interactions at the filter coefficient switching points make the analysis very different for the time-varying case. Analysis and interpretation of time-varying filter banks is complicated by the fact that the tools we would like to use, such as the DTFT and z-transform, are inherently time-invariant. By couching the problem in terms of left and right signal components and the initial conditions associated with them, we have proved that maximally decimated time-varying filter bank analysis/synthesis systems can be exactly reconstructing. We determined that the unknown parameters in the analysis equations (3) and (4) and synthesis equations (6) and (7) are

$$A = M_1$$
$$B = N_1$$
$$C = M_0$$
$$D = N_0$$

$$\tag{24}$$

and that the resulting reconstruction synthesis equations are

$$x_R[n-M_1] = \frac{1}{-\alpha_{M_1}^R} \sum_{\ell=1}^{M_1} \alpha_{M_1-\ell}^R x_R[n+\ell-M_1] + \frac{1}{\alpha_{M_1}^R} \sum_{m=0}^{N_1} \beta_{N_1-m}^R v_R[n+m-N_1] \tag{25}$$

for $0 \leq n < \infty$ with $v_R[n] = v_L[n]$ in the range $-N_1 \leq n \leq -1$ and

$$x_L[n - M_0] = \frac{1}{-\alpha_{M_0}^L} \sum_{\ell=1}^{M_0} \alpha_{M_0-\ell}^L x_L[n + \ell - M_0] + \frac{1}{\alpha_{M_0}^L} \sum_{m=0}^{N_0} \beta_{N_0-m}^L v_L[n + m - N_0] \quad (26)$$

for $-\infty < n \leq -1$.

4.1 Constraints on Switching in the System

This z-domain analysis and the resulting synthesis equations reveal some interesting and important properties of the analysis/synthesis system. To begin, observe that the derivation leading to equation (25) proves that the samples of the input $x[n]$ in the range $-M_1 \leq n \leq \infty$ can be reconstructed using equation (25), where $x[n] = x_R[n]$. Similarly the samples of $x[n]$ in the range $-\infty \leq n < -M_0$ can be reconstructed using equation (26), where $x[n] = x_L[n]$ in this region.

In order to reconstruct all sample values using equations (25) and (26), constraints upon the variables M_0 and M_1 must be imposed. This observation can be drawn from Figure (6) with the following constraint being placed upon M_0 and M_1:

$$M_1 + 1 \geq M_0.$$

If this constraint is not met, the values in between M_0 and M_1 can not be recovered from the reconstruction equations (25) and (26) as shown in Figure (6). There exists a gap of unrecoverable samples in between M_0 and M_1.

Equations (25) and (26) also show that by supplying the original sample values in the transition regions explicitly, the constraint on the separation between switching points can be removed completely. As we saw, switching coefficients at an interval less than or equal to M_1 precludes the recovery of all samples in the region $-M_1 \leq n < 0$. If these missing samples were supplied externally, then reconstruction can proceed without difficulty. Unfortunately, such an approach results in a data increase, i.e. the analysis/synthesis system is no longer maximally decimated.

For convenience of being able to use the conventional unilateral z-transform, the analysis has been given under the assumption that the switching of filters occurs at $n = 0$. But nothing is changed by switching the coefficients at an arbitrary time, $n = n_0$, except for a time shift. All the equations derived are applicable to a system with arbitrary time shift at $n = n_0$. Based on the analysis, it should be clear that these results hold independent of when the filters are switched.

However, the equations reveal limits on how frequent these switching of the filter coefficients can occur within a given interval and on the numerator/denominator orders of the polyphase filters. To illustrate this, consider the example in Figure (6). Equation (25) reconstructs valid
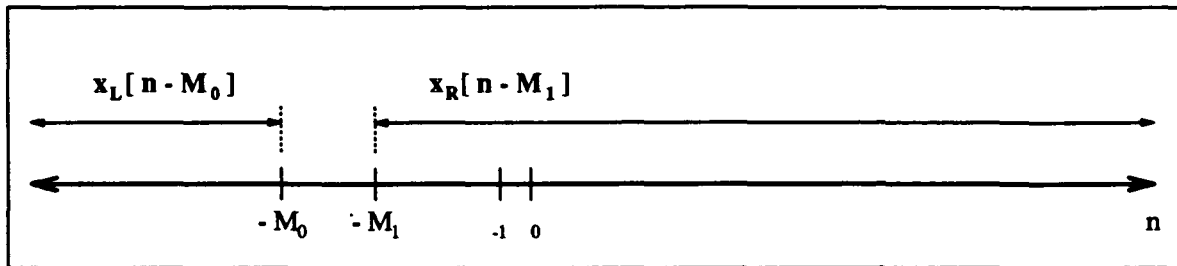
Figure 6: Reconstructing Samples using Equations 25 and 26 Illustrating Constraint on M_0 and M_1

samples of $x_R[n] = x_L[n]$ for $n = -1, -2, ..., -M_1$. These samples are used as initial conditions in equation (26). However, if another switch of coefficients occurs at time $n = K$ where $-M_1 < K < 0$, only K valid samples can be reconstructed from equation (25), the remaining samples in the interval will be erroneous due to the switch in coefficients. Thus, the analysis proves that exact reconstruction can be achieved when the filters are changed at arbitrary intervals provided that the switch points are separated by a number of samples equal to or greater than the numerator order of the associated analysis polyphase filter. Assuming n_i and n_{i+1} are consecutive switch point indices in n, the criterion for exact reconstruction is

$$n_{i+1} - n_i \geq M_1.$$

We hasten to point out that this is an extremely mild restriction in practical applications. This is because the orders of practical recursive polyphase filters tend to be very low. Recursive filters which are first-order allpass polyphase filters can have magnitude characteristics comparable to a 24- or 32-tap QMF. Such filters have extremely good magnitude characteristics and generally provide more than enough stopband rejection with sufficiently narrow transition bands. Because the polyphase filter order is just one in this case, the polyphase filters can be switched every other sample if needed.

4.2 Stability Issue

Another issue to address is stability. It is well known that if the filter coefficients are allowed to change arbitrarily, the system is not guaranteed to be stable. In our case, however, this is not a problem. In the formulation for the recursive time-varying analysis-synthesis system, the general problem is decomposed into piecewise constant coefficient system components, each of which is stable. Since the switch points are separated by M_1 samples, each region (after a switch) that is reconstructed by equation (26) can be represented uniquely by a unilateral z-transform term. In fact, all reconstructed regions that lie between switch points can be represented by separate unilateral z-transforms.

To illustrate this, consider the first-order allpass polyphase filter all-pass polyphase filters

$$P_0(z) = \frac{\alpha - z^{-1}}{1 - \alpha z^{-1}}, \qquad |\alpha| < 1,$$

which we assume to be a filter employed over a finite interval. The corresponding difference equation is

$$y_0[n] = \alpha y_0[n-1] + \alpha x_0[n] - x_0[n-1]$$

and is used to generate all the samples in the interval. The initial conditions for the equation are derived from the output in the previous interval and in general will not be zero. If we take unilateral z-transforms on the above equation, we obtain the transform-domain equation

$$Y_0(z) = \frac{\alpha - z^{-1}}{1 - \alpha z^{-1}} \left[X_0(z) + \frac{\alpha y_0[-1] - x_0[-1]}{\alpha - z^{-1}} \right]$$

where $y_0[-1]$ is the initial condition. Since, the value of α is less than one, the equation output will always be bounded.

The stability is thus completely determined by the locations of the poles of the corresponding transform. That is to say, for stability the poles associated with the analysis polyphase filters should be inside the unit circle and the zeros of the analysis polyphase filters (which become the poles of the synthesis polyphase filters) should be outside the circle.

5   Experiments and Performance Analysis

The analysis presented here used the simple case of a two-band polyphase system to develop the reconstruction equation derivation. Since the result applies to the actual polyphase and inverse polyphase filtering operations, banks with complex-valued channels [11] and an infinite variety of tree structures composed of two-band and/or parallel form filter banks.

Finally, as alluded to in the introduction, time-varying filter banks can improve the subjective and objective performance because of the input dependency of the error characteristics. This is clearly the motivation for the development of time-varying filter banks. It is also a measure by which one can judge its utility.

As an initial gauge of performance, we compare a conventional two-band subband coder and a two-band subband coder with time-varying filter coefficients. A finite length sequence was used as the input — shown in Figure 7 as the solid line. This input is a section of a row taken from the 256 × 256 test image "Lena." In each case, the lowpass channel was coded with 4-bit uniform quantization while the highpass channel was coded with 2 bits. Notice that the conventional subband coder displays ringing (or overshoot-undershoot) distortion at the discontinuities as indicated by the dashed line in Figure 7. However, the other regions of the row are represented well. The magnitude and step response characteristics for $H_0(z)$ used in the conventional subband coder are shown in Figure 8.
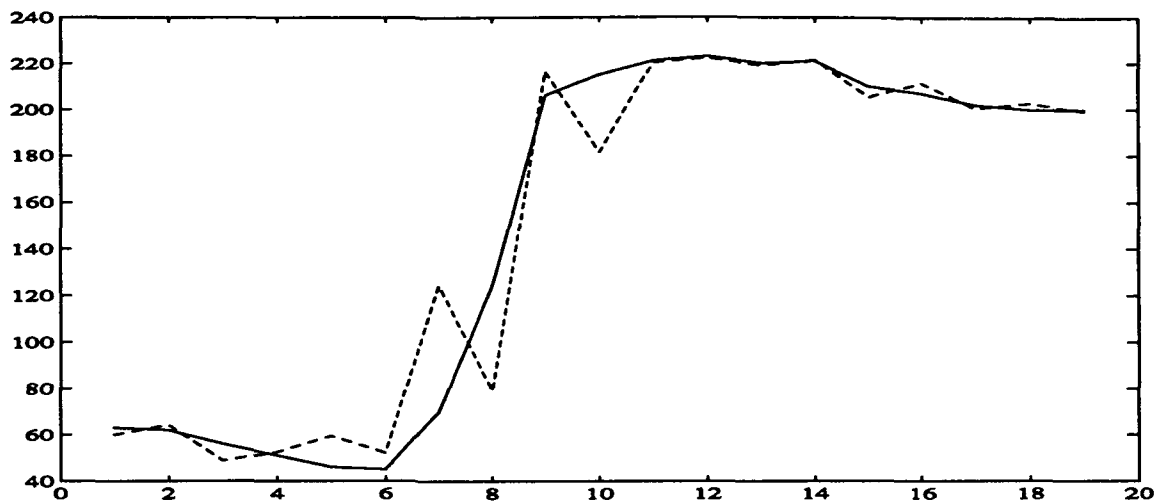
Figure 7: Performance of a two-band subband coder on an image row taken from "Lena." The solid line is the original row. The dashed line is the coded result.
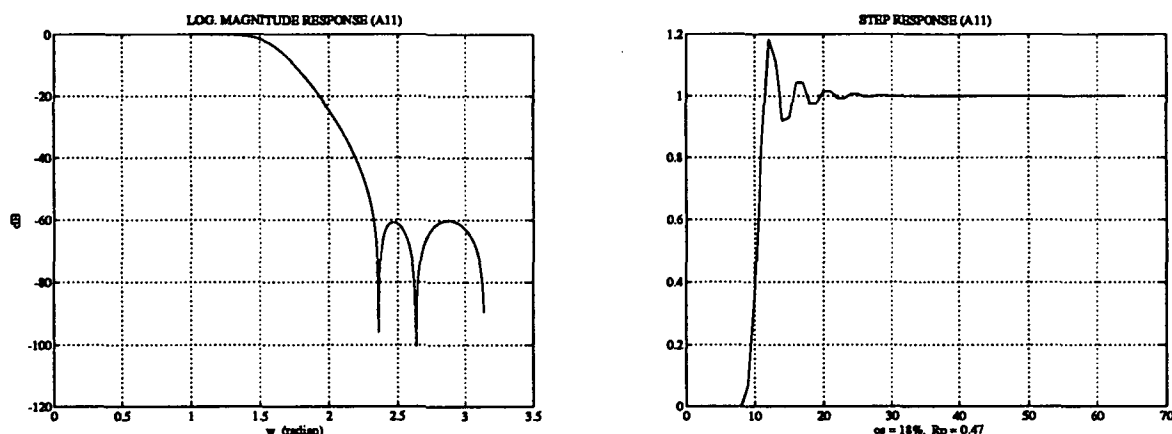

Figure 8: Magnitude and step response for the lowpass filter $H_0(z)$.

The new subband coder with time-varying coefficients employs two filter sets, one with good magnitude response characteristics (i.e. $H_0(z)$ shown in Figure 8) and the other with good step response characteristics. The magnitude and step response characteristics for the latter filter are shown in Figure 9. In the regions of large discontinuity, the filter set with good step response characteristics is used. In other regions, the filter set with good magnitude response characteristics is used. Figure 10 shows the improvement that results for this example.

6   Remarks

Such an approach involves having to convey switching point information to the receiver for reconstruction. This can be done simply by sending side information as was the case in the example or potentially through a procedure based on feedback, the latter of which is presently being studied. For natural images, the amount of side information is negligible. Thus, even with the transmission of side information, this new approach seems attractive.
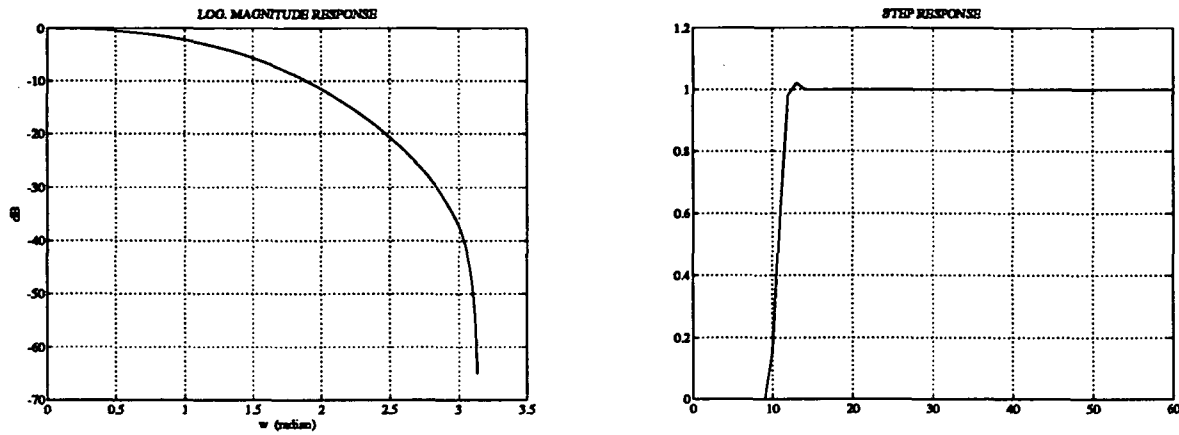
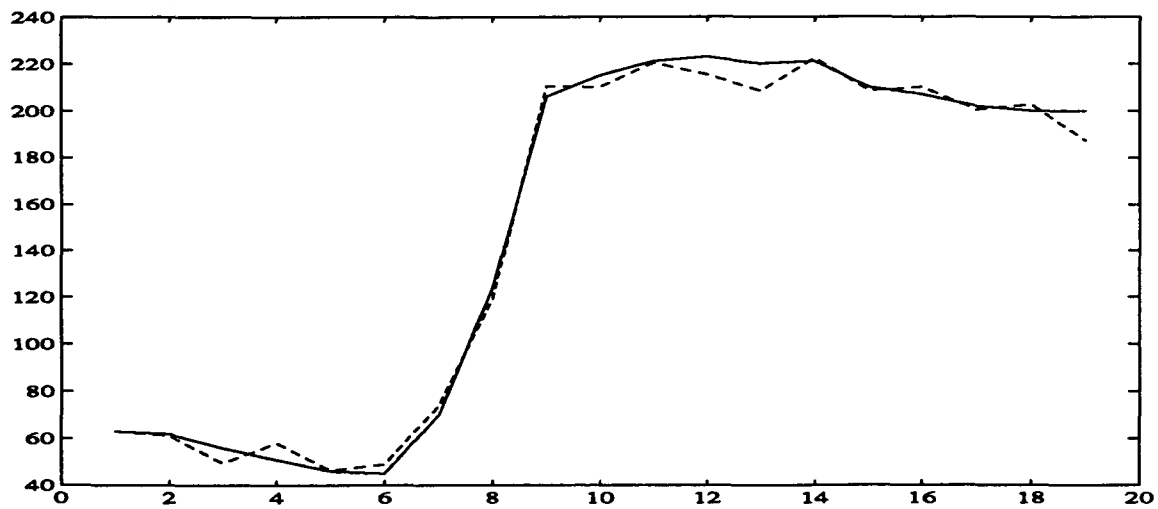Figure 9: Magnitude and step response for the second lowpass filter used in the time-varying filter bank.

Figure 10: Performance of the new subband coder with time-varying coefficients. The solid line shows an image row taken from "Lena." The dashed line is the coded result.

References

[1] J. W. Woods and S. D. O'Neil, "Subband coding of images," *IEEE Trans. Acoust., Speech, Signal Processing*, ASSP–34, pp. 1278–1288, Oct. 1986.

[2] *Subband Image Coding*, (John Woods, Ed.), Kluwer Academic Publishers, Copyright 1991.

[3] K. Nayebi, T. P. Barnwell, and M. J. T. Smith, "Analysis-Synthesis Systems Based on Time Varying Filter Banks," *Int. Conf. on Acoustics, Speech, and Signal Processing*, March 23-26, 1992, vol. IV pp. 617-620.

[4] M. J. T. Smith and S. L. Eddins, "Analysis/synthesis techniques for subband image coding," *IEEE Trans. on Acoustics, Speech, and Signal Processing*, August 1991.

[5] P. Jeanrenaud and M. J. T. Smith, "Recursive multirate image coding with adaptive prediction and finite state vector quantization," *Signal Processing*, May 1990, Vol. 20, No. 1, pp. 25 - 42.

[6] M. J. T. Smith and S. L. Eddins, "Subband coding of images with octave band tree structures," *Proc. IEEE Int. Conf. Acoust., Speech, Signal Processing*, pp. 1382–1385, 1987.

[7] G. Karlsson and M. Vetterli, "Sub-band coding of finite length signals," submitted to *Signal Processing*.

[8] R. H. Bamberger and M. J. T. Smith, "Multirate Filter Bank Preprocessor for Image Compression," *Proc. IEEE Southeastcon*, pp. 890–894, 1989.

[9] R. H. Bamberger and M. J. T. Smith, "Predictive Coding Schemes for Subband Image Coders," *Proc. IEEE Southeastcon*, pp. 872–876, 1989.

[10] J. D. Johnston, "A filter family designed for use in quadrature mirror filter banks," *Proc. IEEE Int. Conf. Acoust. Speech Signal Processing*, pp. 291–294, April 1980.

[11] J. H. Husoy, "Subband Coding of Still Images and Video," Ph.D. Thesis, University of Trondheim, Norway, 1991.

[12] T. Kronander, *Some Aspects of Perception Based Image Coding*, Ph.D. Thesis, Dept. of Electrical Engineering, Linkoping University, Sweden, 1989.

[13] K. Nayebi, T. P. Barnwell, and M. J. T. Smith, "A General Time Domain Analysis and Design Framework for Exactly Reconstructing FIR Analysis/Synthesis Filter Banks," International Symposium on Circuits and Systems, New Orleans, Louisiana, May 1-3, 1990, pp. 2022-2025.

[14] K. Nayebi, T. P. Barnwell, and M. J. T. Smith, "The Time Domain Analysis and Design of Exactly Reconstructing Analysis/Synthesis Filter Banks," International Conference on

Acoustics Speech and Signal Processing, Albuquerque, New Mexico, April 3-6, 1990, pp. 1735-1738.

[15] K. Nayebi, T. P. Barnwell, and M. J. T. Smith, "Analysis-synthesis systems with time-varying filter bank structures," *IEEE Trans. on Acoustics, Speech, and Signal Processing*, pp. IV-617 - IV-620, 1992.

[16] M. J. T. Smith and W. C. Chung, "Adaptive IIR Analysis-Synthesis Filter Banks," *IEEE DSP Workshop*, September 16-19, 1992, Chicago, Illinois.

[17] M. J. T. Smith and W. C. Chung, "Spatially Adaptive IIR Analysis-Synthesis Filter Banks for Image Coding," Asilomar Conference, October, 1992.

[18] J. Husoy and S. Aase, "Image Subband Coding with Adaptive Filter Banks," *SPIE Visual Communications and Image Processing Conference*, November 18-20, 1992.

Appendix: Derivation of Shift Property

The unilateral z-transform is defined as

$$X_R(z) = \sum_{n=0}^{\infty} x[n]z^{-n}.$$

If $x[n]$ is shifted by a positive integer time shift N, and the transform computed, we obtain

$$\sum_{n=0}^{\infty} x[n-N]z^{-n}.$$

Substituting $n = k + N$, results in

$$\sum_{k=-N}^{\infty} x[k]z^{-k-N} = z^{-N} \sum_{k=0}^{\infty} x[k]z^{-k} + z^{-N} \sum_{k=-N}^{-1} x[k]z^{-k}$$

$$= X_R(z)z^{-N} + z^{-N} \sum_{k=-N}^{-1} x[k]z^{-k}.$$

If we let $k = N - \ell$ and substitute, we obtain

$$X_R(z)z^{-N} + \sum_{\ell=0}^{N-1} x[\ell - N]z^{-\ell}.$$

Because this is valid only for integer $N > 0$ we can append the term $u[N - 1]$. For negative shifts, $N < 0$, the transform becomes

$$\sum_{n=0}^{\infty} x[n-N]z^{-n} = \sum_{k=-N}^{\infty} x[k]z^{-k-N} = z^{-N} \sum_{k=0}^{\infty} x[k]z^{-k} - z^{-N} \sum_{k=0}^{-N-1} x[k]z^{-k}$$

$$= X_R(z)z^{-N} - z^{-N} \sum_{k=0}^{-N-1} x[k]z^{-k}u[-N-1]$$

where $u[-N-1]$ restricts N to be less than zero. Combining these results yields

$$x[n-N] \Longleftrightarrow z^{-N}X_R(z) + z^{-N}\sum_{\ell=0}^{N-1} x[\ell - N]z^{-\ell}u[N-1] - z^{-N}\sum_{k=0}^{-N-1} x[k]z^{-k}u[-N-1].$$

For the anti-causal case, the derivation is similar. The transform of the time shifted input is

$$\sum_{n=-\infty}^{-1} x[n-N]z^{-n}.$$

Assuming $N > 0$ and substituting $n = k + N$, results in

$$\sum_{k=-\infty}^{-N-1} x[k]z^{-k-N} = z^{-N} \sum_{k=-\infty}^{-1} x[k]z^{-k} - z^{-N} \sum_{k=-N}^{-1} x[k]z^{-k}$$

$$= X_L(z)z^{-N} - z^{-N}\sum_{k=1}^{N} x[-k]z^{k}$$

For $N < 0$, the transform becomes

$$\sum_{n=-\infty}^{-1} x[n-N]z^{-n} = \sum_{k=-\infty}^{-N-1} x[k]z^{-k-N} = z^{-N} \underbrace{\sum_{k=-\infty}^{-1} x[k]z^{-k}}_{X_L(z)} + z^{-N} \sum_{k=0}^{-N-1} x[k]z^{-k}$$

Combining both results we obtain

$$x[n-N] \Longleftrightarrow z^{-N} X_L(z) - z^{-N} \sum_{\ell=1}^{N} x[-\ell]z^{\ell}u[N-1] + z^{-N} \sum_{\ell=0}^{-N-1} x[\ell]z^{-\ell}u[-N-1]. \qquad (27)$$